PAA-PAMPS Copolymers as an Efficient Tool to Control CaCO$_3$ Scale Formation

Michael Dietzsch,[†,∇,¶] Matthias Barz,[‡,∇,¶] Timo Schüler,[†] Stefanie Klassen,[§] Martin Schreiber,[§] Moritz Susewind,[†] Niklas Loges,[†,◆] Michael Lang,[○] Nadja Hellmann,[∥] Monika Fritz,[⊥] Karl Fischer,[§] Patrick Theato,[#] Angelika Kühnle,[§] Manfred Schmidt,[§] Rudolf Zentel,[*,‡] and Wolfgang Tremel[*,†]

[†]Institut für Anorganische Chemie und Analytische Chemie, [‡]Institut für Organische Chemie, and [§]Institut für Physikalische Chemie, Johannes Gutenberg-Universität, Duesbergweg 10-14, D-55128 Mainz, Germany

[∥]Institut für Molekulare Biophysik, Johannes Gutenberg-Universität, Jakob Welder Weg 26, D-55128 Mainz, Germany

[⊥]Institut für Biophysik, Universität Bremen, Otto-Hahn Allee 1, D-28359 Bremen, Germany

[#]Institut für Technische und Makromolekulare Chemie, Department Chemie, Universität Hamburg, Bundesstraße 45, D-20146 Hamburg, Germany

[∇]Graduate School Materials Science in Mainz, Staudinger Weg 9, D-55128 Mainz, Germany

[○]Mifa AG, Rheinstr. 99, CH-4402 Frenkendorf, Switzerland

S *Supporting Information*

ABSTRACT: Scale formation, the deposition of certain minerals such as CaCO$_3$, MgCO$_3$, and CaSO$_4$·2H$_2$O in industrial facilities and household devices, leads to reduced efficiency or severe damage. Therefore, incrustation is a major problem in everyday life. In recent years, double hydrophilic block copolymers (DHBCs) have been the focus of interest in academia with regard to their antiscaling potential. In this work, we synthesized well-defined blocklike PAA-PAMPS copolymers consisting of acrylic acid (AA) and 2-acrylamido-2-methyl-propane sulfonate (AMPS) units in a one-step reaction by RAFT polymerization. The derived copolymers had dispersities of 1.3 and below. The copolymers have then been investigated in detail regarding their impact on the different stages of the crystallization process of CaCO$_3$. Ca^{2+} complexation, the first step of a precipitation process, and polyelectrolyte stability in aqueous solution have been investigated by potentiometric measurements, isothermal titration calorimetry (ITC), and dynamic light scattering (DLS). A weak Ca^{2+}

induced copolymer aggregation without concomitant precipitation was observed. Nucleation, early particle growth, and colloidal stability have been monitored in situ with DLS. The copolymers retard or even completely suppress nucleation, most probably by complexation of solution aggregates. In addition, they stabilize existing CaCO$_3$ particles in the nanometer regime. In situ AFM was used as a tool to verify the coordination of the copolymer to the calcite (104) crystal surface and to estimate its potential as a growth inhibitor in a supersaturated CaCO$_3$ environment. All investigated copolymers instantly stopped further crystal growth. The carboxylate richest copolymer as the most promising antiscaling candidate proved its enormous potential in scale inhibition as well in an industrial-filming test (Fresenius standard method).
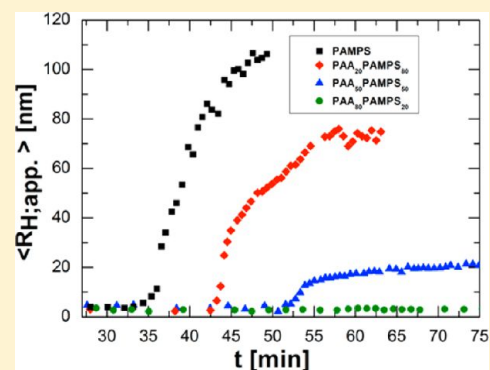
■ INTRODUCTION

Controlling the crystallization of calcium carbonate is of great importance both in academics and industry. First, it is a challenge to understand and control the mineralization process itself.[1−8] The formation of mineral scales leads to significant problems during the washing and cleaning process or in aqueous closed cycle cooling systems.[9−11] Thus, water-soluble polymers which have the ability to complexate ions or adsorb on the particle surface play a major role in the inhibition of scale formation.[12−14] In this context, polycarboxylated polymers are currently used in detergent and cleaner formulations for fabric washing and automatic dishwashing or for pipe protection in industrial water cooling systems.[15] After banning

polyphosphates as detergents for environmental reasons, polycarboxylated polymers such as poly(acrylic acid) (AA), poly[(acrylic acid)-co-(maleic acid)], or polyaspartate became increasingly important in commercial detergents, but they do not perform as well as polyphosphates.[16] During the past 15 years, double hydrophilic block copolymers (DHBCs) have found large interest in academia with respect to their potential as antiscaling agents.[16−18] Typically, they consist of an anchor block, which interacts with the substrate, and a second,

noninteracting block, which renders enhanced solubility. Therefore, DHBCs can stabilize complexes or particles in aqueous solution in a surfactant-like fashion. Although the mechanisms of nucleation and crystal growth control are still a matter of debate, current working models are based on (i) prevention of nucleation through ion complexation, (ii) prevention of nucleation by stabilization of prenucleation clusters,[19,20] and (iii) surface stabilization of precursor particles in the nanometer regime by surface coordination. Their impact on the crystallization process during its early[19–21] and later stages has been investigated for various minerals.[22,23]

Most of the reported DHBCs employed nonionic polyethylene oxide as the solubilizing block. This role is filled by the sulfonate groups of the copolymers reported here. This type of copolymers has been in industrial use for several years (e.g., ALCOGUARD 40-80, ACUSOL 587, ACUSOL 588, Aquatreat 545). Due to its very low pK_a value and strong hydration, the sulfonated side chain of 2-acrylamido-2-methyl-propane sulfonate (AMPS) is a superior solubilizing group over the whole pH range that can stabilize aggregates or particles in solution while the carboxylate groups interact with solvated or surface-bound Ca^{2+} ions. Thus, AA-co-AMPS copolymers are used to control scale formation even under high-ionic-strength conditions. However, these copolymers are commonly prepared by free radical polymerization using chain transfer agents,[24,25] and thus, control about molecular weight, dispersity, and copolymer microstructure is reduced. We have chosen to synthesize AA-co-AMPS copolymers of various compositions via RAFT polymerization,[26–28] since this methodology appears to be a reasonable compromise between better defined polymer structure and facile synthesis in aqueous solution. Additionally, the reported polymerization methodology bears the potential of transfer to industrial scale production.

In this contribution, we describe the influence of these copolymers on the formation of calcium carbonate during various stages of the precipitation process, for example, prenucleation stage, nucleation, early growth, and crystallization stage. The Ca^{2+} complexation, as the first step of a precipitation process, and polyelectrolyte stability in aqueous solution have been investigated by potentiometric measurements, ITC and DLS. Nucleation, early particle growth and colloidal stability have been monitored in situ with DLS. In situ AFM was used as a tool to obtain mechanistic information about the polymer coordination on the crystal surface. The most promising copolymer was further evaluated in a crystallization study and in an industrial-filming test (Fresenius standard method).

■ EXPERIMENTAL SECTION

Materials. Unless specified otherwise, all chemicals were reagent grade and obtained from Aldrich. The 2-acrylamido-2-propane sulfonate monomer solution was obtained from Lubrizol. Acrylic acid was distilled prior to polymerization. All chemicals were used without further purification. The polymerizations were performed in deionized water (Millipore) adjusted to pH 6.

Polymer Synthesis and Characterization. *CTA Synthesis.* The chain transfer agent was synthesized following McCormick and Lowe.[27] In a 1000 mL reaction flask, 22.9 g of carbon disulfide and 2.0 g of tetrabutylammonium hydrogensulfate were dissolved in 150 mL of dodecane under nitrogen atmosphere. The reaction flask was equipped with a reflux condenser, dropping funnel, and cooling unit. To this solution, 168 g of sodium hydroxide solution (50 wt %) was added slowly in order to keep the temperature between 20 and 30 °C. After a reaction time of 30 min, 43.6 g of acetone and 89.6 g of chloroform

were added to the solution whose color turned yellowish afterward. The solution was stirred overnight under nitrogen atmosphere. During this period, a yellow to brownish solid precipitated from the solution. The precipitate was dissolved again by adding 500 mL of deionized water. The organic and aqueous phases were separated, and the aqueous phase was acidified with concentrated HCl. After acidification, a yellow solid precipitated. The solution was cooled down to complete the precipitation. The yellow solid was removed from the solution and dried. For purification, the product was transferred to toluene and this suspension was stirred overnight. The toluene was removed, and the final product was dried in a vacuum oven. The yield was 21.3% with respect to carbon disulfide. ^1H NMR (CDCl$_3$) δ/ppm: 1.67 (6H, s). ^{13}C NMR (CDCl$_3$) δ/ppm: 220.12 (1C), 173.59 (2C), 56.70 (3C), 25.63 (4C). FD-MS: calculated for $C_9H_{14}O_4S_3$ 282.0; found 282.1.

Synthesis of PAA-PAMPS Copolymers. Acrylic acid and the Na-AMPS solution from Lubrizol were introduced into a 200 mL Schlenk tube. A volume of 20 mL of deionized water was added to this solution. Afterward, S,S'-bis-α,α'-dimethyl-α''-acetic acid trithiocarbonate and 4,4-azobis(cyanopentanoic acid) were added to the solution. The resulting solution was degassed in three vacuum thaw cycles. The polymerization was carried out overnight at 70 °C and stopped by cooling the solution in an ice bath and exposure to air. Subsequently, the solvent was removed, and the final product was dried in a vacuum oven. A yellowish granulate was yielded. (yield 98%) ^1H NMR (D$_2$O) δ/ppm: 3.89 (m 2H, s), 2.25 (n 1H, br s), 1.81 (n 2H, br s), 1.68 (n 2H, br s), 1.38 (m 6H, s).

Polymer Characterization. ^1H NMR spectra were obtained with a 300 MHz instrument using a FT-spectrometer from Bruker and analyzed using the ACDLabs 6.0 software. The polymers were dried at 40 °C overnight under vacuum and afterward submitted to gel permeation chromatography (GPC). Gel permeation chromatography (GPC) was performed in aqueous ammonium formiate solution ($c = 0.1$ M). Calibration was done using poly(acrylic acid) standards from PSS. The flow rate was 1 mL/min at a temperature of 25 °C.

In order to determine the copolymer composition, the polymers were freeze-dried over 3 days to remove condensed water. Approximately 1 mM in monomer units (indicated by the composition determined via NMR) of the polymer was dissolved in 50 mL of 1 M NaCl solution in order to screen electrostatic forces on the polyelectrolyte surface. The solution was then titrated with 0.1 M NaOH solution, so that the number of AA groups and hence the number of AMPS groups could be calculated. The latter was already deprotonated because the sodium salt of 2-acrylamido-2-propane sulfonic acid (Na-AMPS) had been used during the polymerization reaction.

Determination of the Calcium Complexation. *Ca^{2+} Selective Electrode.* The condensation of calcium ions to the PAA-PAMPS polymers of various compositions was quantified by measuring the Ca^{2+} activity with a pH 340/ION meter (manufactured by WTW) and a CA 60 calcium selective combination electrode (manufactured by Schott Instruments). The calcium electrode was calibrated by measuring the voltage of Ca^{2+} solutions of different concentrations, ranging from 5×10^{-4} to 1.5×10^{-2} mol/L, in the presence [KCl] = 0.08 mol/L in order to guarantee comparable ionic strengths in standard and analyte solutions. To 50 mL of an aqueous solution, which contained 1 mM in monomer units of the copolymer and 1 mM CaCl$_2$, a 0.1 M NaOH solution was added in increments of 10 μL to deprotonate the AA groups.

Isothermal Titration Calorimetry. The binding of Ca^{2+} to PAA$_{83}$-PAMPS$_{19}$ and PAA$_{20}$-PAMPS$_{80}$ was investigated by ITC (VP-ITC MicroCal Northhampton, MA). Sample and reference cells contained a volume of 1.4287 mL of the polyelectrolyte solution (16.5 mM of PAA$_{80}$-PAMPS$_{20}$ (A) or 11 mM of PAA$_{20}$-PAMPS$_{80}$ (B), pH= 7.5) and water. A concentration of 200 mM (A) or 40 mM (B) of CaCl$_2$ was titrated in 3 μL increments with an injection syringe (250 μL total volume), which simultaneously served as a stirrer at a rate of 200 rpm. Dilution heat effects were determined by titrating CaCl$_2$ in water and water in the polyelectrolyte, respectively, and subtracted from the detected measured heat in the complexation experiment. All data was acquired at a constant temperature of 20 °C. By integration of the heat

power over time, the removed or supplied heat was calculated. Data analysis was based on a model for n identical binding sites provided by the instrument's software.

Precipitation and Crystallization Experiments. *Precipitation by Hydrolysis of Carbonate Esters[29] Traced with Dynamic Light Scattering.* Three solutions were prepared: 50 mL of a 30 mM of $CaCl_2$ and 30 mM DEC solution, 50 mL of a 24 mM NaOH solution, and 50 mL of a solution containing a 3-fold excess of the polymer mass, set to pH = 7. The polymer concentrations were adjusted in a way that all polymer solutions contained the same number of monomer units. A concentration of 0.5 g/L (2.2 mM) for the Na-PAMPS polymer was chosen as reference value, and the respective concentrations of the copolymers were adjusted to this value accordingly. In this way, differences in the antiscaling behavior depending on the copolymer composition could be investigated best.

The three solutions were mixed under stirring. The addition of the NaOH solution marks the starting point of the measurement. Approximately 2 mL of the mixture was then filtered through a Millpore GS filter with a pore size of 0.22 μm into a cylindrical quarz-glass cuvette (Hellma, no. 540.135) with an outer diameter of 20 mm.

DLS experiments were performed at T = 298 K with a commercial ALV setup using a frequency doubled Nd:YAG laser (λ = 532 nm and P = 750 mW) in at Θ = 90°. The DLS-detector system consists of a single mode fiber with a fiber coupler (Schäfter +Kirchhoff - SuK, Hamburg), an ALV static and dynamic enhancer (ALV GmbH, Langen, Germany), a fiber-beam splitter, two avalanche photodiodes (SPCMAQR-14, Perkin-Elmer), and an ALV7004/fast multiple tau digital correlator (ALV GmbH). The correlation time was typically set to 30 s; however, in the case of fast particle growth, it was decreased to 10−20 s in order to reduce fluctuations of the baseline.

A biexponential function was fitted to the field correlation function g_1

$$g_1(q, \tau) = a_1\, e^{-D_1 q^2 \tau} + a_2\, e^{-D_2 q^2 \tau} \qquad (1)$$

$$\langle D_{app} \rangle = \frac{a_1 D_1 + a_2 D_2}{a_1 + a_2} \qquad (2)$$

and the hydrodynamic radius was calculated according to the Stokes−Einstein equation

$$\langle R_{H;app} \rangle = \frac{kT}{6\pi\eta D_{app}} \qquad (3)$$

Crystallization Experiments with the $(NH_4)_2CO_3$ Gas Diffusion Method. Crystallization experiments were performed with the standard $(NH_4)_2CO_3$ diffusion method. Spectrosil glass slides were cleaned in acid piranha solution (H_2O_2/H_2SO_4 1:1), rinsed with water and ethanol, further cut into smaller pieces, and placed in a microreaction tube (1 mL, Eppendorf), which contained a 1 mL solution of 10 mM $CaCl_2$ and 5 mM PAA_{80}-$PAMPS_{20}$. Two holes were punched in the lid with a needle and the tubes were put in a desiccator. The experiment was started by placing a Petri dish with 7 g of crushed ammonium carbonate at the bottom of the desiccator. The Petri dish was covered with needle punched parafilm. The reference experiments were carried out simultaneously in the same desiccator but without additive. The sample was taken out after 60 min, carefully rinsed with water and ethanol and then dried in a nitrogen flow. The resulting crystals were examined with a laser scanning microscope (Keyence VK-8710).

Atomic Force Microscopy (AFM). Atomic force microscopy (AFM) images were taken in the intermittent contact mode (tapping mode) using a commercial instrument (Bruker MultiMode V with Nanoscope V controller) that has been optimized for operation in liquids.[30] The calcite samples used for AFM imaging were of optical quality from Korth KristalleGmbH (Kiel, Germany). To minimize contaminations, all calcite samples were cleaved immediately before inserting them into the fluid cell (standard closed fluid cell from Bruker). We cleaved the samples by gently scoring a line parallel to the edge of the crystal with a scalpel, a recipe known to produce flat (104) cleavage planes.[31] The influence of the polymers on the growth of calcite was then

investigated by exposing the freshly cleaved calcite first to a 1.85 supersaturated $CaCO_3$ solution for a few minutes, followed by replacing said solution with a 1.85 supersaturated solution containing the respective polymer.

As force sensors, we used gold-coated, p-doped silicon cantilevers (PPPNCHAuD from Nanosensors, Neuchâtel, Switzerland) with an eigenfrequency of about 150 kHz, a spring constant of about 40 N/m, and a Q value of around 8 in Milli-Q water (Millipore GmbH, Schwalbach, Germany).

Industrial Antifilming Test. The tests were performed according to the Fresenius testing procedure for the evaluation of calcium carbonate film formation. A Miele G651 SC Plus dishwasher was used. The machine was loaded with three plates of China black (Bauscher), 3 plates of glass black (Luminarc), 3 plates of plastics (SAN) blue 24 cm (Waca = 1 pan in stainless steel, 2 knives, 2 glasses "Paris" (Schott/Zwiesel) = Schott, 2 glasses "Saft classic"; (Stölzle) = Stölzle, 3 glasses, "Islande" Whisky (arcoroc) = whisky; and 3 glasses "Mondial" (Schott/Zwiesel) = red wine. The polymer containing compact powder formulation was prepared according to the industrial standards. The tests were performed in the presence of ballast soil and a water hardness of 21°d using the program Universal Plus 65°C. The evaluation was performed after 5 and 10 cycles 30 min after completion of each washing cycle. After the crockery is completely dried, the filming effect was evaluated visually in a "black box" under defined light conditions (halogen light).

■ RESULTS AND DISCUSSION

Polymer Synthesis. In this work, we studied the influence of PAA-PAMPS copolymers and their composition on the precipitation of $CaCO_3$. To this end, we synthesized various copolymers by the RAFT polymerization method according to Scheme 1.

Scheme 1. Synthesis of the Poly(acrylic acid *co*-2-acrylamido-2-propane sulfonate) Copolymers via RAFT Polymerization
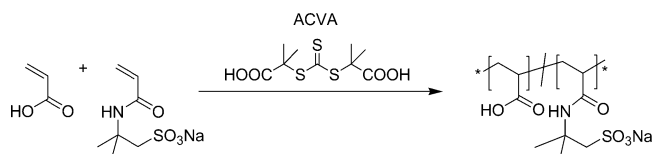
The copolymers differ in constitution and molecular weight. The AA/AMPS ratio was varied from 80:20 to 20:80 (the numbers represent the fraction of the total number of monomer units in percent), and the molecular weights were set to be in the range from 5000 to 12 000 g/mol. We observed slight variations between the calculated molecular weight and the one estimated by GPC, which are, in all probability, related to the fact that the GPC was calibrated with PAA standards. Nevertheless, control over the molecular weight and molecular weight distribution was achieved. In general, the polydispersity index (PDI) was between 1.1 and 1.3 depending on the AA/AMPS ratio in the copolymer. The copolymers used in this study are listed in Table 1.

The composition of the copolymer was calculated from the NMR spectra by comparing the integral from 3.2 to 3.4 ppm (AMPS side chain) with the integral of the backbone C−H from 2.0 to 2.5 ppm. From the ratio of these integrals we determined the content of AMPS in the copolymer (see the Supporting Information). Additionally, the composition of the copolymers was determined by titration with NaOH.

For higher AMPS contents, we observed discrepancies in the ratios determined by NMR and titration (Table 1). Due to

Table 1. Characterization of Synthesized Poly(acrylic acid co-2-acrylamido-2-propane sulfonate) Copolymers

polymer	AA/AMPS ratio$_{(calc)}$	AA/AMPS ratio[a]	AA/AMPS ratio[b]	Mn$_{(calc)}$	Mn[c]	M_w[c]	PDI[c]
P1	80:20	82:18	83:17	6000	5000	6200	1.22
P3	50:50	52:48	60:40	6000	6100	7500	1.23
P5	20:80	24:76	31:69	6000	6200	8300	1.34
P7	0:100	0:100		12 000	9500	14 700	1.56

[a]Determined by ^{1}H NMR [b]Determined by titration. [c]Determined by GPC in aqueous ammonium formate solution (c = 0.1 mol/L) using acrylic acid standards from PSS.

signal broadening in NMR, which hinders an accurate integration, we considered the ratios determined via titration to be more reliable and used them for adjusting concentrations in monomer units per volume.

The copolymerization parameters were determined according to the Mayo−Lewis method (see the Supporting Information). For the monomer mixture AMPS/AA (r_1/r_2), we determined r values of r_1 = 1.37 and r_2 = 0.58, indicating that AMPS prefers to polymerize with monomers of the same type. Thus, for small and moderate molar AMPS/AA ratios blocklike copolymers are formed.

Calcium Complexation. It is well-known that polycarboxylates strongly bind calcium ions, which often leads to aggregation and even precipitation at high calcium concentrations.[32−34] The latter case was nicely examined by Huber et al. who followed the Ca^{2+}-induced collapse of PAA chains with the help of DLS and SLS.[35,36] This effect becomes more pronounced with increasing chain length. At the outset, the precipitation process is characterized by a contraction of the coil, most probably through conformational changes and Ca^{2+} bridging, followed by a distinct coil to globe transition. Although the polymer captures a fraction of the calcium ions from solution and thus reduces the effective supersaturation during precipitation, it cannot stabilize emerging calcium carbonate clusters or particles anymore. In a detailed calorimetric analysis, Antonietti et al. investigated the binding of Ca^{2+} to various polycarboxylates (NaPAA, NaPAsp, Sokalan) and detected in all cases an endothermic heat flow, whose magnitude decreased with increasing ratio of Ca^{2+} ions and carboxylate binding sites r = [Ca^{2+}]/[COO[−]] until precipitation occurred (r = 0.31 for Ca-PAA, r = 0.24 for Ca-Sokalan and r = 0.66 for Ca-PAsp).[37] The driving force is the release of Ca^{2+} coordinating water molecules which results in a strong entropy gain.

Potentiometric measurements were performed to investigate the calcium binding to the PAA-PAMPS copolymers. All solutions were normalized to 1 mM of Ca^{2+} and 1 mM in monomer units of the polymer irrespective of the type (Figure 1). Unlike the acrylic acid groups, the AMPS units are already deprotonated prior to addition of any NaOH. Thus, AMPS-rich copolymers are strongly charged at the beginning of the experiment. The sulfonate groups do not bind any Ca^{2+} ions at all, since the concentration of unbound Ca^{2+} ions equals the total Ca^{2+} ions available in the beginning of the experiment. Addition of NaOH and subsequent deprotonation of the carboxylate groups induces Ca^{2+} binding and therefore decreases the amount of free calcium in solution, until a slightly substoichiometric ratio of Ca^{2+} ions is bound.

Our ITC measurements (Figure SI 4 and Table SI 1, Supporting Information) also show an endothermic heat flow which is, however, significantly lower for PAA$_{20}$-PAMPS$_{80}$ ($\Delta H°_{bind}$ = 7.2 kJ/mol) compared to PAA$_{80}$-PAMPS$_{20}$ ($\Delta H°_{bind}$ = 14.0 kJ/mol) and PAA (17.0 kJ/mol). This is
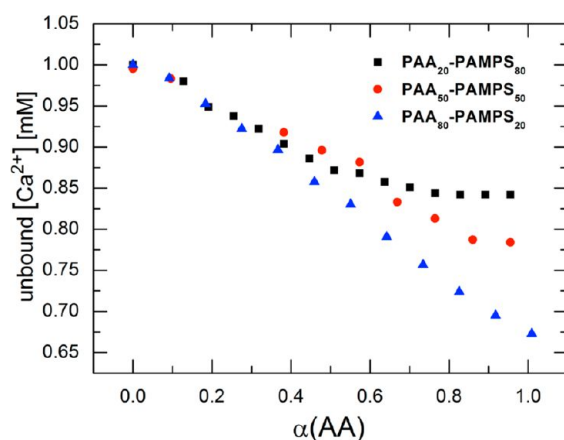

Figure 1. Concentration of free calcium ions in dependence of the degree of neutralization α of the AA units in the copolymer. All solutions contained 1 mM in total monomer units of the polymer and 1 mM Ca^{2+}.

attributed to the lower number of AMPS units in PAA$_{20}$-PAMPS$_{80}$ in combination with an increased solubility of the Ca^{2+}-polyelectrolyte complexes attributed to the AMPS. This was also observed by Antonietti et al.,[37] who found a more exothermic binding behavior for NaPAsp compared to NaPAA and explained it by the more hydrophilic properties of the backbone of the PAsp polyelectrolyte, which is also reflected by a shift of the precipitation limit toward higher calcium loads.

DLS measurements were carried out to determine a possible aggregation or eventual precipitation of the copolymer with the highest AA content (PAA$_{80}$-PAMPS$_{20}$) in the presence of Ca^{2+} in comparison to a classical polycarboxylate (PMAA; M_w = 1200 g/mol, PDI < 1.2). PAA$_{80}$-PAMPS$_{20}$ was chosen because it was the copolymer with the lowest PAMPS content and therefore closest in composition to a pure polycarboxylate. Only small aggregates were formed in the presence of the copolymer, which lead to the appearance of weak scattering intensities. Therefore, a calcium dependent study of the aggregation could not be carried out. A ratio of [Ca]/[PAA$_{80}$-PAMPS$_{20}$] = 2.5 however yielded correlation functions at a scattering angle of θ = 30°, which could be fitted with a biexponential fit to a hydrodynamic radius of 10 nm (Figure SI 2, Supporting Information). In contrast, Na-PMAA formed much larger aggregates at the same [Ca]/[polymer] ratio. Extrapolation to $\theta = q = 0$ yields a hydrodynamic radius of R_H = 95 nm (Figure SI 3, Supporting Information). Unlike PMAA, the copolymers do not precipitate, even at high calcium loads ([Ca^{2+}] > 100 mM) (data not shown). In summary, the copolymers can bind Ca^{2+} ions and weakly aggregate by crosslinking through intermolecular Ca^{2+} bridges, but they do not precipitate because the low Ca^{2+} affinity of the AMPS moieties retains a sufficiently large solubility. Thus, the copolymers can

act as stabilizing surface ligands for $CaCO_3$ aggregates in the postnucleation stage.

Nucleation and Early Growth. The precipitation method by Faatz et al.,[29] which is based on the hydrolysis of dialkyl carbonate with NaOH, was used to study the influence of the additives on nucleation and early growth. In this case, carbonate is generated under homogeneous conditions, which allows monitoring the precipitation process with DLS. We used diethyl carbonate [DEC] as carbonate precursor, and concentrations of $[CaCl_2]$ = [DEC] = 10 mM and [NaOH] = 8 mM were found to discriminate the influence of the different polymers best. All solutions were adjusted to the same number of monomer units (2.2 mM).

Figure 2 displays the growth curves for pure PAMPS and three copolymers. The reference experiment carried out in the
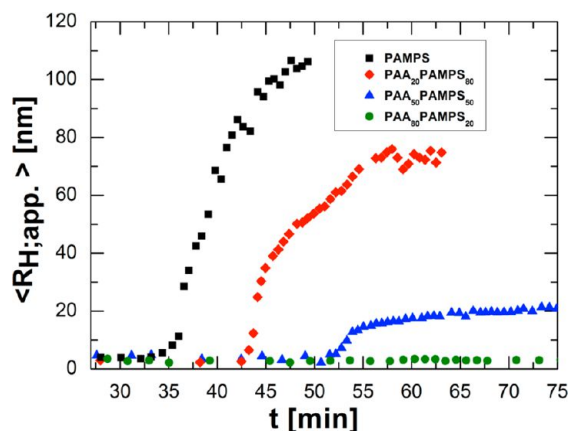

Figure 2. Apparent hydrodynamic radius obtained from in situ DLS experiments starting with $[CaCl_2]$ = [DEC] = 10 mM and [NaOH] = 8 mM in the presence of various polymers. T = 298 K, θ = 90°. All polymer concentrations were adjusted to the same number of monomer units (2.2 mM).

absence of additives (Figure SI 5, Supporting Information) indicates nucleation after 32 min with subsequent particle growth to a particle size of well over R_H = 300 nm. Considering that all runs were carried out at a constant angle of θ = 90°, only apparent values for the hydrodynamic radius are obtained which leads to underestimation of the true (inversely) z-averaged particle size due to the contribution of the particle form factor.

In the presence of PAMPS, PAA_{20}-$PAMPS_{80}$, and PAA_{50}-$PAMPS_{50}$, nucleation was retarded. The early postnucleation stage is characterized by a linear increase of the apparent hydrodynamic radius followed by a convergence toward a saturation value. In the saturation limit, the particle size of copolymer aggregates remains static for hours; only a slight increase in the scattering intensity was observed, which can tentatively be ascribed to a densification and crystallization of the particles. Retardation of nucleation as well as particle stabilization became more pronounced with increasing PAA fraction. Interestingly, the copolymer with the highest number of PAA units, PAA_{80}-$PAMPS_{20}$, completely inhibits nucleation in this experimental setup and hence demonstrates the highest antiscaling potential. The strong inhibition of nucleation by this polymer cannot solely be ascribed to simple Ca^{2+} ion complexation because in terms of total Ca^{2+} binding, the three copolymers do not differ much, compared to the starting concentration of $[Ca^{2+}]$ = 10 mM. Furthermore, recent results for PAA homopolymers, which precipitated under similar conditions, showed only a slight delay or even a promotion of nucleation, depending on their molecular mass.[38] Cölfen et al. came to similar conclusions by titrating $CaCl_2$ into a carbonate buffer in the presence of various additives. They concluded that (i) the role of ion complexation has been overestimated and (ii) the key step in retarding nucleation is the stabilization of prenucleation clusters by additives which prevent their aggregation and subsequent nucleation.[19,20]

Additional crystallization experiments with the best performing polymer PAA_{80}-$PAMPS_{20}$, were carried out, using the $(NH_4)_2CO_3$ diffusion method.[39] Representative images are shown in Figure 3. In this setup, nucleation and crystallization are not completely inhibited. However, compared to the reference experiment (Figure 3a), which led to the formation of calcite crystals with a size of about 20 μm, the additive appears to reduce the nucleation rate, reflected by the particle number, strongly decreases the crystallite sizes, and thus prevents the formation of macroscopic amounts of $CaCO_3$ (Figure 3b).

In Situ Atomic Force Microscopy. In order to obtain a better understanding of the growth inhibiting effect from a molecular point of view, in situ AFM imaging was performed on freshly cleaved calcite samples in the absence and presence of polymer. For the sake of clarity, AFM images are either shown as the topography (z) or as the derivation of the topography raw data (dz/dx). Figure 4a−f show a series of representative AFM images of calcite (104) taken as a reference in 1.85 supersaturated $CaCO_3$ solution in the absence of
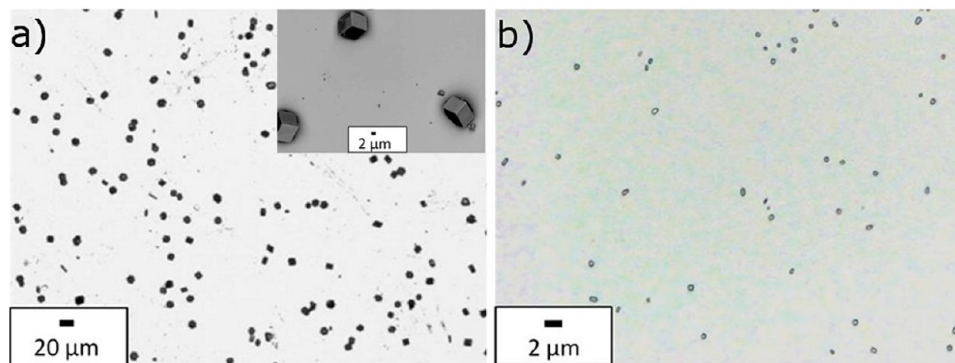

Figure 3. Crystallization experiments performed using the $(NH_4)_2CO_3$ method, $[CaCl_2]$ = 10 mM, stopped after 1 h. (a) Reference experiment in the absence of additives; (b) in the presence of $PAA_{80}PAMPS_{20}$ (5 mM).
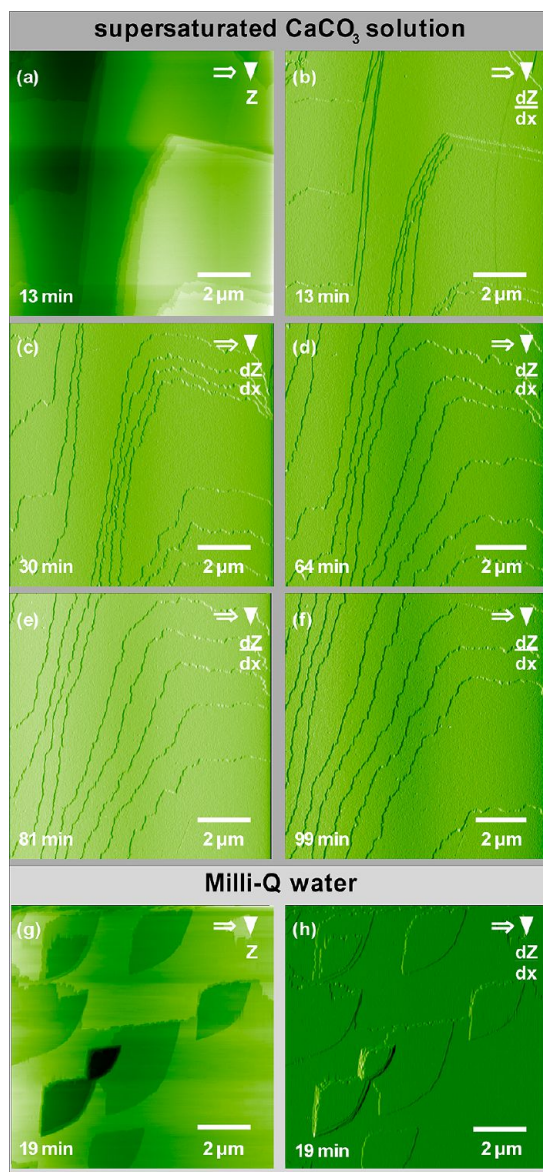
Figure 4. Time-dependent series of tapping mode AFM images taken on calcite (104). (a−f) Images taken in 1.85 supersaturated CaCO$_3$ solution after 13, 30, 64, 81, and 99 min showing the in situ growth. (g, h) Tapping mode images taken on calcite (104) in Milli-Q water after 19 min.

polymer. The step edges are not stable but change in time. This is a well-known observation when imaging calcite in supersaturated CaCO$_3$ solution, reflecting the in situ growth of calcite. In contrast, characteristic, diamond-shaped etch pits appear when imaging calcite (104) in pure Milli-Q water, as shown in Figure 4g and h,[40,41] reflecting the dissolution until the solution reaches its saturation level.

This behavior changed drastically in the presence of PAA and PAMPS solutions. When calcite was imaged in a 1.85 supersaturated solution containing 4.5 mM PAA (M_w = 15 000 g/mol), the well-known etch pits developed immediately after introducing the calcite sample into the solution (Figure 5a) despite using a supersaturated CaCO$_3$ solution. This observation can be readily explained by the fact that PAA forms a complex with the calcium cations in solution, effectively reducing the ion concentration and, thus, inducing calcite dissolution.
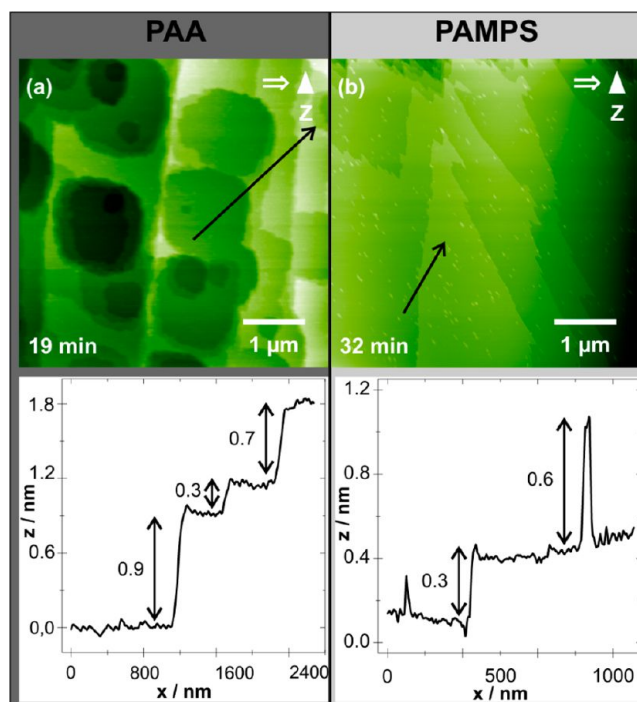

Figure 5. Tapping mode AFM topography images taken on calcite (104) in 1.85 supersaturated CaCO$_3$ solution in the presence of polymer. (a) PAA: image taken 19 min after adding the solution. (b) PAMPS: image taken 32 min after adding the solution.

A fundamentally different situation was obtained however when imaging calcite in a 4.5 mM PAMPS solution (M_w = 15 000 g/mol) in supersaturated CaCO$_3$ (Figure 5b). In this case, no etch pits were formed because (i) a supersaturated CaCO$_3$ solution was used and (ii) PAMPS does not bind Ca^{2+} as shown by potentiometry. Instead, adsorbates with an apparent height of approximately 0.7 ± 0.1 nm exist on the surface, exhibiting a needlelike shape. Compared to calcite (104) imaged in the absence of polymer, the step edges shown here reveal a meandered shape. Interestingly, the step edges appear free from adsorbates, indicating that the step edges do not act as nucleation sites for polymer adsorption. As AFM shows the coordination of this purely sulfonated polymer onto the crystal surface and also in situ DLS revealed a weak stabilizing effect, we conclude that the PAMPS block does not only account for solubilization (its function in a typical DHBC) but interacts to some extent with the CaCO$_3$ particles or crystals as well.

Next, the impact of the copolymer solutions was investigated. Again the solutions were normalized to the same number of monomer units. A series of images taken in the presence of 4.5 mM PAA$_{20}$-PAMPS$_{80}$ (a−f) and PAA$_{50}$-PAMPS$_{50}$ (g−l) in a supersaturated CaCO$_3$ solution is shown in Figure 6. These images reveal no change in the step edge configuration even after 90 min of exposure, clearly demonstrating the growth-inhibiting effect of the copolymers. A zoom into a stepped region exhibits adsorbates with an apparent height of 0.4 ± 0.1 nm and 0.7 ± 0.1 nm (Figure 6f and l). In clear contrast to the reference samples, these adsorbates are mainly observed to decorate the step edges.

A different situation was revealed when the fraction of PAA in the copolymer was further increased. A series of images taken in the presence of 4.5 mM PAA$_{80}$-PAMS$_{20}$ is shown in Figure 6m−r. As for the two other copolymers, calcite crystal growth is
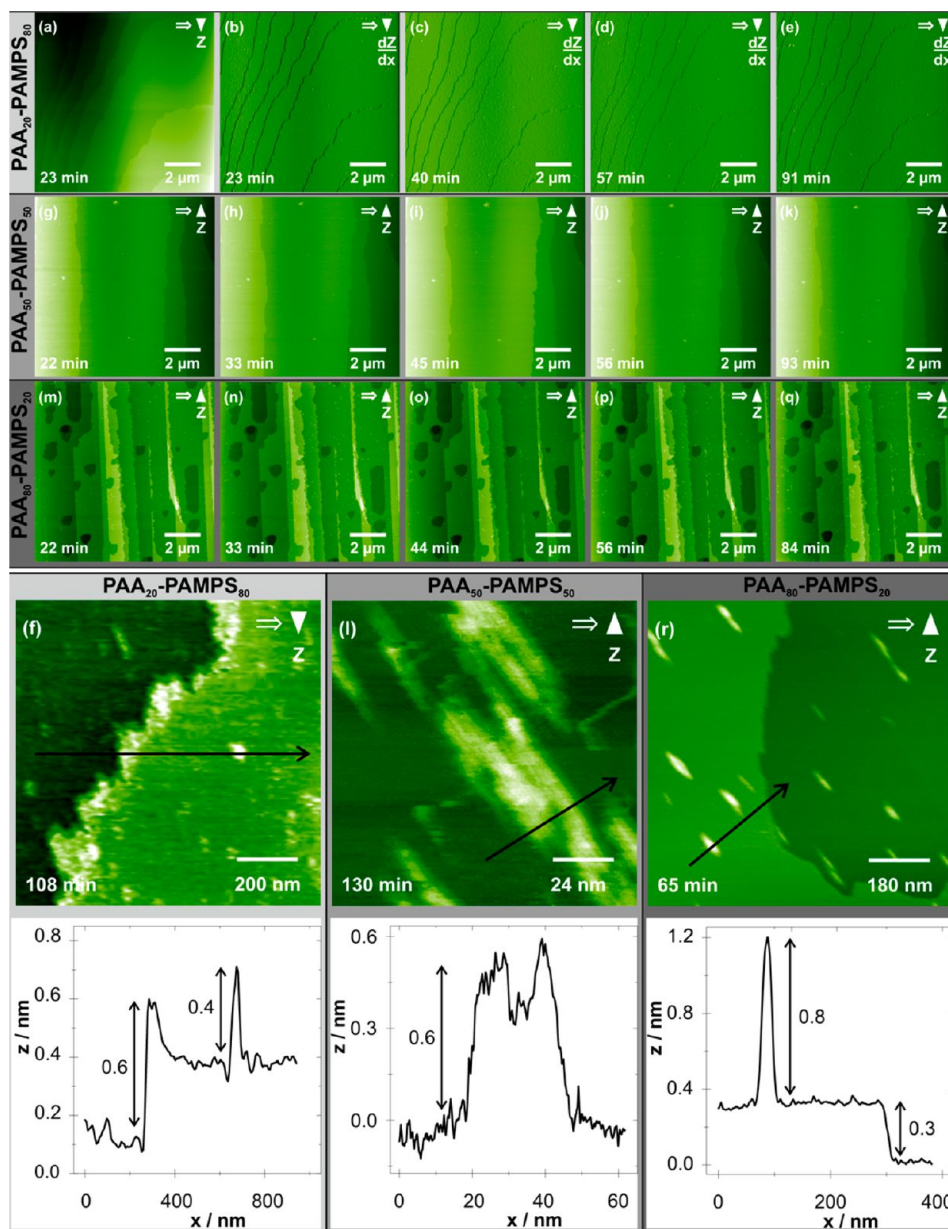
Figure 6. Time-dependent series of tapping mode AFM topography taken on calcite (104) in the presence of PAA-PAMPS copolymers. (a–f) PAA_{20}-$PAMPS_{80}$: images taken 23, 40, 57, and 91 min after adding the solution to the calcite sample, respectively. (g–l) PAA_{50}-$PAMPS_{50}$: Images taken 22, 33, 45, 56, and 93 min after adding the solution to the calcite sample, respectively. (m–r) PAA_{80}-$PAMPS_{20}$: Images taken after 22, 33, 44, 56, and 84 min after adding the solution to the calcite sample, respectively. Line profiles are extracted as indicated by arrows in (f), (l), and (r).

stopped effectively. However, in sharp contrast to the structures obtained in the presence of PAA_{20}-$PAMPS_{80}$ and PAA_{50}-$PAMPS_{50}$, etch pits exist on the surface already a few minutes after introducing the polymer solution, which indicates that the solution became undersaturated at this polymer concentration. Compared to the pure PAA solution, the etch pits obtained in the presence of PAA_{83}-$PAMS_{17}$ solution do not show the characteristic diamond shape. Instead, meandered edges appear similar to those observed for the pure PAMPS solution. Moreover, the surface is covered by needlelike adsorbates that resemble the structures obtained in the presence of PAA_{50}-$PAMPS_{50}$. A zoom reveals adsorbates with an apparent height of 0.7 ± 0.1 (Figure 6r).

Industrial Antifilming Tests. The performance of the most promising copolymer PAA_{80}-$PAMPS_{20}$ was examined in a standard industrial testing setup. The antifilming test was performed according to the Fresenius standard method. In this test, several commercial glasses and dishes were placed in a dishwasher, ballast soil and the polymer containing formulations were added, and the cleaning program was started (see Experimental Section).

We have chosen commercial copolymers comprising carboxylated and sulfonated units such as ALCOGUARD 4080, Aquatreat 545, or ACUSOL 588 to compare the antifilming performance in an industrial testing setup. In the first test reported here, we compared ALCOGUARD 4080 with PAA_{80}-$PAMPS_{20}$, both of which are copolymers of comparable composition and molecular weight. Both polymers were tested in standard phosphate containing and phosphate free compact powder formulations for machine dishwashing. It turned out that already after 5 washing cycles a difference in the performance of the polymer was clearly apparent. The
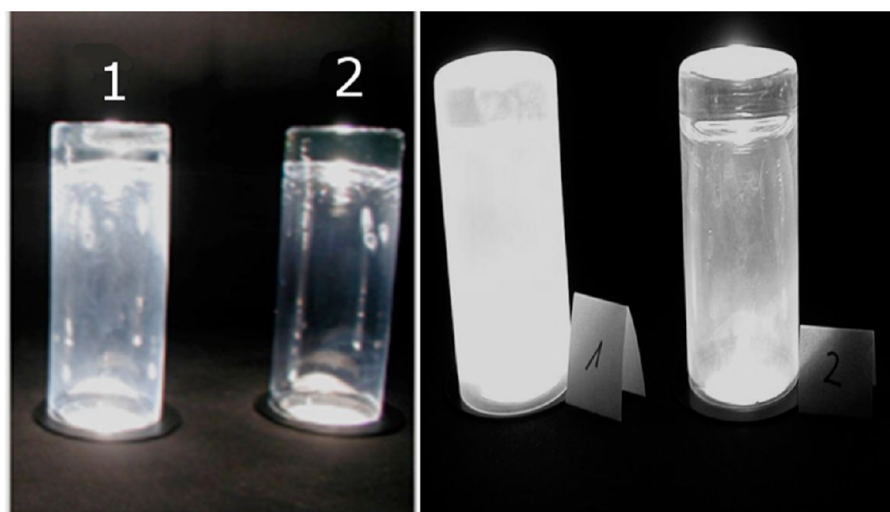
Figure 7. Representative image of polymer performance in an antiscaling filming test (Fresenius standard method) after 10 washing cycles. The glasses have been washed with standard formulations containing either the commercial polymer ALCOGUARD 4080-G (1) or PAA_{80}-$PAMPS_{20}$ (2). The left image shows phosphate containing formulations, and the right image shows phosphate free formulations.

difference in the antifilming performance was even more pronounced after 10 washing cycles. Whereas the commercial polymer failed in preventing film formation, the PAA_{80}-$PAMPS_{20}$ copolymer suppressed filming effectively (see Figure 7) in phosphate free as well as phosphate containing formulations.

The performance of the polymer PAA_{80}-$PAMPS_{20}$ was independent of the type of glass. The performance of the PAA_{80}-$PAMPS_{20}$ copolymer was in all cases superior to the commercially available product of comparable composition and molecular weight.

CONCLUSION

PAA-PAMPS blocklike copolymers of different compositions and molar masses of approximately 10 000 g/mol were synthesized in a one step synthesis via RAFT polymerization and investigated in terms of their antiscaling potential during the different stages of calcium carbonate formation. Calcium ions only bind to the carboxylate groups in substoichiometric amounts. They induce a weak aggregation of the copolymers ($d_H \approx 20$ nm) but do not lead to a precipitation, even at very high calcium loads, very different from the cases of polycarboxylates or polyphosphates. $CaCO_3$ nucleation and early growth could be traced by DLS. It could be demonstrated that the copolymers (i) retard nucleation and (ii) stabilize nanoscaled $CaCO_3$ particles in the postnucleation stage. Both effects become more pronounced with increasing PAA content of the copolymer. Remarkably, the carboxylate-richest copolymer PAA_{80}-$PAMPS_{20}$ was able to suppress $CaCO_3$ formation virtually completely. It showed a very good performance in the Fresenius industrial antifilming test and proved itself an effective antiscaling agent. The strong inhibition of nucleation by the carboxylate-rich copolymers cannot be explained by Ca^{2+} ion complexation only; in addition, a stabilization of solution aggregates must be assumed. In situ AFM measurements on the macroscopic calcite (104) face in a supersaturated $CaCO_3$ solution clearly demonstrated that the copolymers instantly inhibit further crystal growth. This can be explained by the fact that the copolymers adsorb onto the step edges and presumably also lower the interfacial energy. From the DLS and AFM results, it can be derived that the highly charged AMPS block contributes to the particle stabilization, not only by accounting for solubility but also by interacting with the particle or crystal surface.

ASSOCIATED CONTENT

ⓢ Supporting Information

^{1}H NMR spectrum of the poly(acrylic acid *co*-2-acrylamido-2-propane sulfonate) copolymer (Figure S1); dynamic light scattering of the Ca-PAA-PAMPS aggregation, experimental details, and correlation function for the Ca^{2+} mediated aggregation of PAA_{80}-$PAMPS_{20}$, (Figure S2); diffusion coefficients of the Ca^{2+}-PMAA aggregates (Figure S3); isothermal titration calorimetry for Ca^{2+}-copolymer complexation, measured heat for the titration of PAA_{20}-$PAMPS_{80}$ solution (pH = 7.5) $CaCl_2$, and the titration of PAA_{80}-$AMPS_{20}$ solution (pH = 7.5) with $CaCl_2$ (Figure S4); in situ dynamic light scattering monitoring $CaCO_3$ nucleation and growth, apparent hydrodynamic radius from DLS experiments (Figure S5); thermodynamic data and stoichiometry obtained from the ITC measurement (Table SI); experimental details for in situ atomic force microscopy. This material is available free of charge via the Internet at http://pubs.acs.org.

AUTHOR INFORMATION

Corresponding Author
*E-mail: tremel@uni-mainz.de (W.T.); zentel@uni-mainz.de (R.Z.).

Present Address
◆N.L.: BASF Construction Chemicals GmbH, Dr.-Albert-Frank-Str. 32, D-83308 Trostberg, Germany

Author Contributions
¶M.D. and M.B. both have equally contributed.

Notes
The authors declare no competing financial interest.

study was funded by the Deutsche Forschungsgemeinschaft (DFG) within the priority program 1415.

■ REFERENCES

(1) Lahav, M.; Leiserowitz, L. The effect of solvent on crystal growth and morphology. *Chem. Eng. Sci.* **2001**, *56*, 2245−2253.

(2) Estroff, L. A.; Hamilton, A. D. At the interface of organic and inorganic chemistry: Bio-inspired synthesis of composite materials. *Chem. Mater.* **2001**, *13*, 3227−3235.

(3) Xu, A.-W.; Dong, W.-F.; Antonietti, M.; Cölfen, H. Polymorph Switching of Calcium Carbonate Crystals by Polymer-Controlled Crystallization. *Adv. Funct. Mater.* **2008**, *18*, 1307−1313.

(4) Meldrum, F. C. Calcium carbonate in biomineralisation and biomimetic chemistry. *Int. Mater. Rev.* **2003**, *48*, 187−224.

(5) Dey, A.; With, G. de; Sommerdijk, N. A. J. M. *In situ* techniques in biomimetic mineralization studies of calcium carbonate. *Chem. Soc. Rev.* **2010**, *39*, 397−409.

(6) Sommerdijk, N. A.; Cölfen, H. Lessons from Nature— Biomimetic Approaches to Minerals with Complex Structures. *MRS Bull.* **2010**, *35*, 116−121.

(7) Gower, L. B. Biomimetic model systems for investigating the amorphous precursor pathway and its role in biomineralization. *Chem. Rev.* **2008**, *108*, 4551−4627.

(8) De Yoreo, J. J.; Vekilov, P. G. Principles of crystal nucleation and growth. *Rev. Mineral.* **2003**, *54*, 57−93.

(9) Rieger, J.; Hadicke, E.; Rau, I.; Boeckh, D. A rational approach to the mechanisms of incrustation inhibition by polymeric additives. *Tenside, Surfactants, Deterg.* **1997**, *34*, 430−435.

(10) Patnaik, P. *Handbook of inorganic chemicals*; McGraw-Hill: New York, 2003.

(11) Lopez-Sandoval, E.; Vazquez-Lopez, C.; Zendejas-Leal, B.; Ramos, G.; San Martin Martinez, E.; Munoz Aguirre, N.; Reguera, E. Calcium carbonate scale inhibition using the "allotropic cell" device. *Desalination* **2007**, *217*, 85−92.

(12) Amjad, Z., Ed. *Water Soluble Polymers*; Kluwer Academic Publishers: Boston, 2002.

(13) Nancollas, G. H.; Kazmierczak, T. F.; Schuttringer, E. Controlled Composition Study of Calcium Carbonate Crystal Growth: The Influence of Scale Inhibitors. *Corrosion* **1981**, *37*, 76−81.

(14) Ketrane, R.; Saidani, B.; Gil, O.; Leleyter, L.; Baraud, F. Efficiency of five scale inhibitors on calcium carbonate precipitation from hard water: effect of temperature and concentration. *Desalination* **2009**, *249*, 1397−1404.

(15) Weber, H.; Ettl, R.; Tropsch, J. Dishwasher Detergent Formulations Comprising A Mixture of Hydrophobically Modified Polycarboxylates. US Patent 0234265, 2010.

(16) Cölfen, H. Double-Hydrophilic Block Copolymers: Synthesis and Application as Novel Surfactants and Crystal Growth Modifiers. *Macromol. Rapid Commun.* **2001**, *22*, 219−252.

(17) Yu, S.-H.; Cölfen, H. Bio-inspired crystal morphogenesis by hydrophilic polymers. *J. Mater. Chem.* **2004**, *14*, 2124−2147.

(18) Mann, S. The Chemistry of Form. *Angew. Chem., Int. Ed.* **2000**, *39*, 3392−3406.

(19) Gebauer, D.; Cölfen, H.; Verch, A.; Antonietti, M. The Multiple Roles of Additives in CaCO₃ Crystallization: A Quantitative Case Study. *Adv. Mater.* **2009**, *21*, 435−439.

(20) Verch, A.; Gebauer, D.; Antonietti, M.; Cölfen, H. How to control the scaling of CaCO3: a "fingerprinting technique" to classify additives. *Phys. Chem. Chem. Phys.* **2011**, *13*, 16811−16820.

(21) Guillemet, B.; Faatz, M.; Gröhn, F.; Wegner, G.; Gnanou, Y. Nanosized amorphous calcium carbonate stabilized by poly(ethylene oxide)-*b*-poly(acrylic acid) block copolymers. *Langmuir* **2006**, *22*, 1875−1879.

(22) Marentette, J. M.; Norwig, J.; Stöckelmann, E.; Meyer, W. H. Crystallization of CaCO₃ in the presence of PEO-*block*-PMAA copolymers. *Adv. Mater.* **1997**, *9*, 647−651.

(23) Antonietti, M.; Breulmann, M.; Göltner, C. G.; Cölfen, H.; Wong, K. K. W.; Walsh, D.; Mann, S. Inorganic/organic mesostructures with complex architectures: precipitation of calcium phosphate in the presence of double-hydrophilic block copolymers. *Chem.—Eur. J.* **1998**, *4*, 2493−2500.

(24) Seok, C. M.; Young-Kee, O.; Kee-Heon, C.; Hyun-Chang, K.; Sang-Woon, K. Powder Detergent Granule Containing ACIDIC Water-Soluble Polymer. US Patent 0137185, 2010.

(25) Gautier, F.; Shulman, J.; Weinstein, B.; Keenan, A.; Duccini, Y. Method for the inhibition of (poly)phosphate scale. Eur. Pat. Appl. 0877022B1, 1998.

(26) Moad, G.; Rizzardo, E.; Thang, S. H. Living Radical Polymerization by the RAFT Process. *Aust. J. Chem.* **2005**, *58*, 379.

(27) McCormick, C. L.; Lowe, A. B. Aqueous RAFT polymerization: recent developments in synthesis of functional water-soluble (co)-polymers with controlled structures. *Acc. Chem. Res.* **2004**, *37*, 312−325.

(28) Moad, G.; Rizzardo, E.; Thang, S. H. Radical addition fragmentation chemistry in *polymer* synthesis. *Polymer* **2008**, *49*, 1079−1131.

(29) Faatz, M.; Gröhn, F.; Wegner, G. Amorphous Calcium Carbonate: Synthesis and Potential Intermediate in Biomineralization. *Adv. Mater.* **2004**, *16*, 996−1000.

(30) Rode, S.; Stark, R.; Lübbe, J.; Tröger, L.; Schütte, J.; Umeda, K.; Kobayashi, K.; Yamada, H.; Kühnle, A. Modification of a commercial AFM for low-noise, high-resolution FM imaging in liquid environment. *Rev. Sci. Instrum.* **2011**, *82*, 73703.

(31) Tröger, L.; Schütte, J.; Ostendorf, F.; Kühnle, A.; Reichling, M. Concept for support and cleavage of brittle crystals. *Rev. Sci. Instrum.* **2009**, *80*, 63703.

(32) Balz, M.; Therese, H. A.; Li, J.; Gutmann, J. S.; Kappl, M.; Nasdala, L.; Hofmeister, W.; Butt, H.-J.; Tremel, W. Crystallization of Vaterite Nanowires by the Cooperative Interaction of Tailor-Made Nucleation Surfaces and Biologically Inspired Polymers. *Adv. Funct. Mater.* **2005**, *15*, 683−688.

(33) Loges, N.; Therese, H. A.; Graf, K.; Nasdala, L.; Tremel, W. Probing Cooperative Interactions of Tailor-Made Nucleation Surfaces and Macromolecules: A Bio-inspired Route to Hollow Micrometer-Sized Calcium Carbonate Particles. *Langmuir* **2006**, *22*, 3073−3080.

(34) Pipich, V.; Balz, M.; Wolf, S.; Tremel, W.; Schwahn, D. Nucleation and Growth of CaCO₃ Mediated by the Egg-White Protein Ovalbumin: A Time-Resolved in-situ Study Using Small-Angle Neutron Scattering. *J. Am. Chem. Soc.* **2008**, *130*, 6879−6892.

(35) Huber, K. Calcium-Induced Shrinking of Polyacrylate Chains in Aqueous Solution. *J. Phys. Chem.* **1993**, *97*, 9825−9830.

(36) Schweins, R.; Huber, K. Collapse of sodium polyacrylate chains in calcium salt solutions. *Eur. Phys. J. E* **2001**, *5*, 117−126.

(37) Sinn, C. G.; Dimova, R.; Antonietti, M. Isothermal Titration Calorimetry of the Polyelectrolyte/Water Interaction and Binding of Ca²⁺: Effects Determining the Quality of Polymeric Scale Inhibitors. *Macromolecules* **2004**, *37*, 3444−3450.

(38) Liu, J.; Pancera, S.; Boyko, V.; Gummel, J.; Nayuk, R.; Huber, K. Impact of sodium polyacrylate on the amorphous calcium carbonate formation from supersaturated solution. *Langmuir* **2012**, *28*, 3593−3605.

(39) Albeck, S.; Weiner, S.; Addadi, L. Polysaccharides of Intracrystalline Glycoproteins Modulate Calcite Crystal Growth In Vitro. *Chem.—Eur. J.* **1996**, *2*, 278−284.

(40) Arvidson, R. S.; Ertan, I. E.; Amonette, J. E.; Luttge, A. Variation in calcite dissolution rates: a fundamental problem? *Geochim. Cosmochim. Acta* **2003**, *67*, 1623−1634.

(41) Britt, D. W.; Hlady, V. In situ AFM imaging of calcite etch pit morphology changes in undersaturated and HEDP-poisonde solutions. *Langmuir* **1997**, *13*, 1873−1876.